JACS
JOURNAL OF THE AMERICAN CHEMICAL SOCIETY
pubs.acs.org/JACS
Article

CO_2 Photoreduction on Metal Oxide Surface Is Driven by Transient Capture of Hot Electrons: *Ab Initio* Quantum Dynamics Simulation

Weibin Chu, Qijing Zheng, Oleg V. Prezhdo, and Jin Zhao*

Cite This: *J. Am. Chem. Soc.* 2020, 142, 3214–3221
Read Online

ABSTRACT: The most critical bottleneck in CO_2 photoreduction lies in the activation of CO_2 to form an anion radical, $CO_2^{\bullet-}$, or other intermediates by the photoexcited electrons, because CO_2 has a high-energy lowest unoccupied molecular orbital (LUMO). Taking rutile TiO_2(110) as a prototypical surface, we use time-dependent *ab initio* nonadiabatic molecular dynamics simulations to reveal that the excitation of bending and antisymmetric stretching vibrations of CO_2 can sufficiently stabilize the CO_2 LUMO below the conduction band minimum, allowing it to trap photoexcited hot electrons and get reduced. Such vibrational excitations occur by formation of a transient $CO_2^{\bullet-}$ adsorbed in an oxygen vacancy. CO_2 can trap the hot electrons for nearly 100 fs and dissociate to form CO within 30−40 fs after the trapping. We propose that the activation of the CO_2 bending and antisymmetric stretching vibrations driven by hot electrons applies to other CO_2 reduction photocatalysts and can be realized by different techniques and material design.

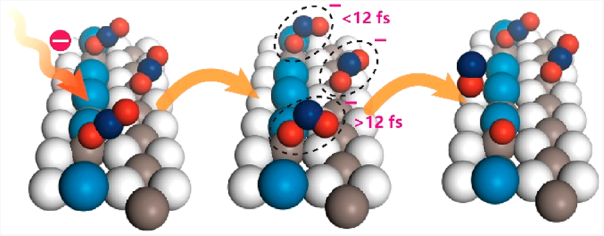

1. INTRODUCTION

Motivated by the constant depletion of finite fossil resources and visible global warming induced by CO_2, the discovery of renewable energy alternatives has become one of the most important scientific challenges in recent decades.[1−4] This has prompted the development of sustainable processes to generate fuels and chemical feedstock from water and CO_2 using solar energy, which is analogous to photosynthesis in plants and also known as "artificial photosynthesis". Compared with H_2, which is generated from H_2O splitting, carbon-based fuels allow for better integration into the existing energy infrastructure. These fuels can be accessed by the photoreduction of CO_2.

Compared with H_2O splitting, the photoreduction of CO_2 is more complex and challenging.[5−9] Photoreduction of CO_2 mainly encompasses the following elementary steps: (i) photon absorption and excited carrier generation; (ii) activation of CO_2 to form an anion radical, $CO_2^{\bullet-}$, or other intermediates by the photoexcited electrons; (iii) dissociation of the C−O bond, involving the participation of protons and electron transfer, generating different products; and (iv) desorption of reduced products from the active sites.[8,9] Among these four steps, the most critical bottleneck lies in the activation of CO_2.[7,8,10−12] CO_2 is a stable and chemically inert molecule with a closed-shell electronic configuration and linear geometry. The addition of a single electron induces a bending of the molecule because of the repulsion between the added electron and the free electron pairs on the oxygen atoms. The bending geometry increases the repulsion between these free electron pairs, which contributes to a high energy of the lowest unoccupied molecular orbital (LUMO) of CO_2. Therefore, the single-electron reduction of CO_2 has a strongly negative electrochemical potential of −1.9 V versus the normal hydrogen electrode.[13] Consequently, almost no semiconductor can provide a sufficiently high energy to transfer a single photoexcited electron to a free CO_2. This remains the most important obstacle to the photoreduction of CO_2. To understand how to decrease the negative electrochemical potential, i.e., to stabilize the LUMO of CO_2 close to or lower than the conduction band minimum (CBM) of the semiconductor, is the critical step to break through the bottleneck of CO_2 photoreduction.

In this report, taking the rutile TiO_2(110) surface as a prototypical system, we have studied photoexcited electron-induced CO_2 reduction on a metal oxide surface by using time-dependent *ab initio* nonadiabatic molecular dynamics (NAMD) simulations. We have found that the excitation of two specific vibrations, i.e., the bending and antisymmetric stretching modes of the CO_2 molecule, can sufficiently decrease the energy of the CO_2 LUMO, making it lower than the CBM of TiO_2 and enabling it to trap the photoexcited hot electrons. The process can be realized by the formation of a transient $CO_2^{\bullet-}$ with bent geometry through the photoexcitation of one electron to the LUMO of CO_2 (as schematically shown in Figure 1a, step 1). If the lifetime of $CO_2^{\bullet-}$ is longer than 12 fs, with the help of oxygen vacancy

Received: December 10, 2019
Published: January 22, 2020

https://dx.doi.org/10.1021/jacs.9b13280
J. Am. Chem. Soc. 2020, 142, 3214−3221

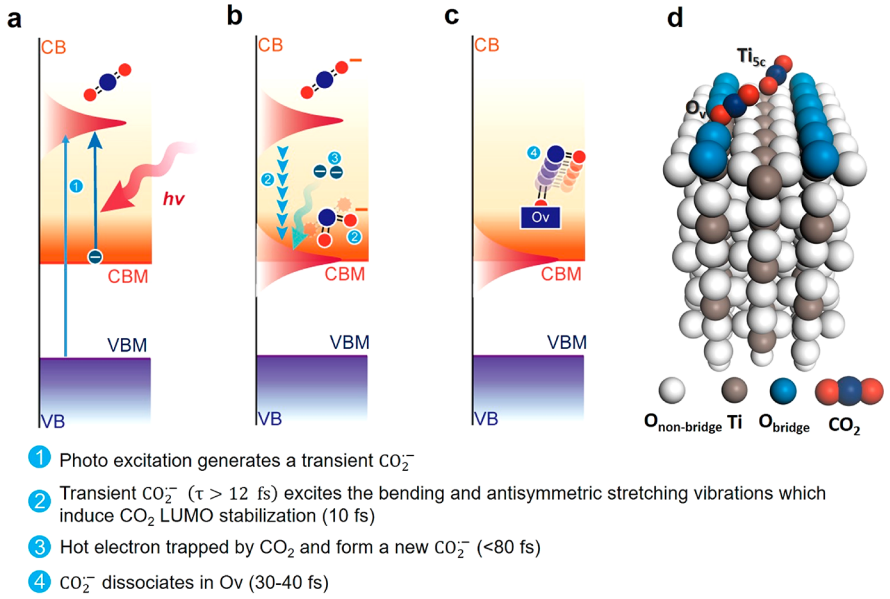

Figure 1. Diagram of CO_2 photoreduction on the TiO_2 surface. The four steps of CO_2 photoreduction and the corresponding time scales are schematically indicated in (a)−(c). (d) Schematic showing the CO_2 molecule adsorbed in the O_V and Ti_{5C} sites on the TiO_2(110) surface.

(O_V), the excitation of the bending and antisymmetric stretching modes will stabilize the LUMO of CO_2 below the CBM within 10 fs, and such electronic state alignment can be kept for longer than 100 fs (step 2 in Figure 1b). Within this time period, CO_2 can trap the hot electrons on a surface with a time scale of 80 fs (step 3 in Figure 1b) and dissociate to form CO within 30−40 fs after trapping the hot electron (step 4 as indicated schematically in Figure 1c). Our results suggest that the excitation of the bending and antisymmetric stretching vibrations can adequately stabilize the LUMO of CO_2, and thus, it plays a vital role in the photoreduction of CO_2 on TiO_2. We propose that the conclusion in this report is widely applied to metal oxides in general, as well as to other semiconductors, which provides important guidance to design photocatalysts with high efficiency for CO_2 reduction.

2. SIMULATION METHODOLOGY

The *ab initio* NAMD study uses density functional theory (DFT) as implemented in the Vienna ab initio simulation package (VASP) to carry out the static and *ab initio* molecular dynamics (MD) calculations.[14−16] The DFT calculations employ the projector augmented wave (PAW) method[17,18] and the Perdew−Burke−Ernzerhof (PBE) exchange-correlation functional,[19] and account for van der Waals (vdW) interactions using DFT-D3.[20] Additionally, we use the VDW-DF correction to verify our results, observing no obvious differences from results obtained with DFT-D3 (Figure S1). An energy cutoff of 450 eV is used for the plane-wave basis sets. A 2×1 supercell with five layers of TiO_2 describes the CO_2/TiO_2 system. To assess the finite size effects, we further used a larger 3×2 supercell to simulate the photoreduction process, and we found no distinct differences (Figure S2a). The bottom layer Ti and O dangling bonds are saturated with pseudo-hydrogens with nuclear charges of +1.25 and +0.75 e, similar to the protocol of Kowalski and co-workers.[21] Due to the self-interaction error in DFT, the electronic bandgap is usually underestimated in metal oxides. However, our previous studies on TiO_2 indicate that alignment of the relevant energy levels at the molecule/TiO_2 interface are affected much less.[22] To confirm this point, we have compared the density of states of CO_2 adsorbed in O_V on the TiO_2(110) surface using DFT and DFT+U (U = 4.5 eV) and have observed only minor differences (Figure S3). A good description for the electronic structure of the system is obtained by sampling the Brillouin zone only at the gamma point.[22] After the geometry optimization, we used velocity rescaling to bring the system's temperature to 100 K; next, initial structures were randomly sampled at 100 K followed by a 2 ps microcanonical *ab initio* MD. A time step of 0.5 fs was used for all the MD.

As we discussed in the Introduction, the addition of a single electron induces bending of the CO_2 molecule. However, bending geometry is not the ground state for neutral CO_2, nor it is the ground state of the CO_2/TiO_2 system. Thus, ground-state MD is not sufficient to study the photoreduction of CO_2. We use the impulsive two-state (I2S) model[23−26] implemented in the MD calculations (see Supplemental Methods for details) to simulate the electron-induced dissociation of CO_2. To account for the excited state, the $CO_2^{\bullet-}$ is modeled by the anionic pseudopotential method,[27] in which one 1s electron is excited from the core part and placed in the LUMO of CO_2 (see Supplemental Methods for details). To simulate the transient $CO_2^{\bullet-}$, the MD trajectory is obtained by evolving the system on the $CO_2^{\bullet-}/TiO_2$ potential energy surface for a short period of time (τ) and, afterward, with the retention of positions and momenta, back to the ground state of CO_2/TiO_2. The pseudopotential approach to simulate the anionic state in this study has led to many successes in previous works on chemical kinetics.[23−26,28]

To investigate the excited carriers' dynamics, which govern the lifetime of $CO_2^{\bullet-}$, we use the *ab initio* NAMD simulations performed using the Hefei-NAMD code[22,29,30] within the time-dependent Kohn−Sham (TDKS) framework.[29] It is a mixed quantum-classical method, in which the nuclei are treated as classical particles based on *ab initio* MD and the electrons are simulated within the quantum framework using the TDKS equation and surface hopping. Thus, the electronic−vibrational coupling can be considered in a time-dependent manner. Using the I2S MD trajectory, the NAMD results are based on averaging over 10 different initial configurations. For each chosen structure, we sample 10^4 trajectories for 100 fs. Along with the reduction process, the weakly coupled adiabatic states would suffer strong state crossing problems, which may lead to artificial long-range charge or energy transfer. To avoid this trivial crossing, we apply a method similar to that proposed by Linjun Wang and co-authors[31,32] (see Supplemental Methods for details). The electronic wave function is propagated in the diabatic representation, and then the hopping probability is corrected with accurate wave function coefficients in the adiabatic representation obtained through the representation transformation technique. In order to avoid the

https://dx.doi.org/10.1021/jacs.9b13280
J. Am. Chem. Soc. 2020, 142, 3214−3221

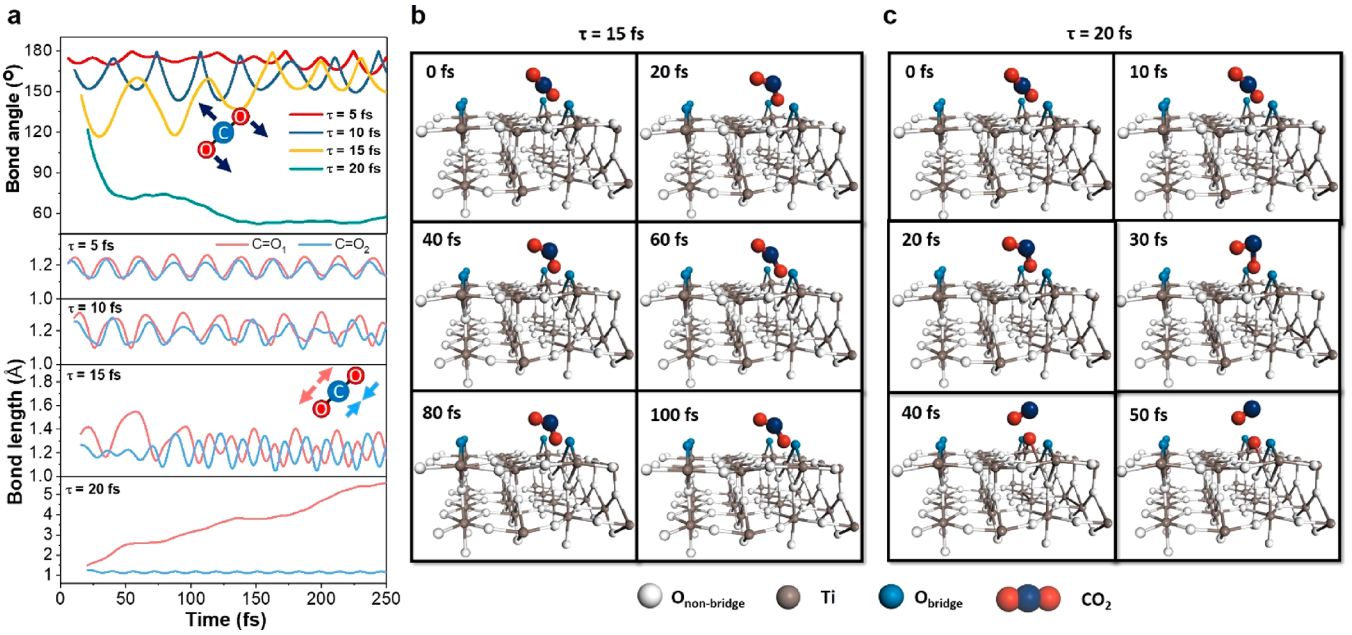

Figure 2. Specific vibrational mode excitations by the formation of transient $CO_2^{\bullet-}$ with the adsorption in O_v on the TiO_2(110) surface. (a) O═C═O bond angle and bond length evolution with different $CO_2^{\bullet-}$ lifetimes. Two different C═O bonds (C═O1 and C═O2) are indicated with the red and blue lines, respectively. (b, c) Snapshots of the atomic structures during the MD trajectory for $CO_2^{\bullet-}$ with different τ. Only one specific trajectory is shown here; more trajectories and the average time scale are offered in Table S1.

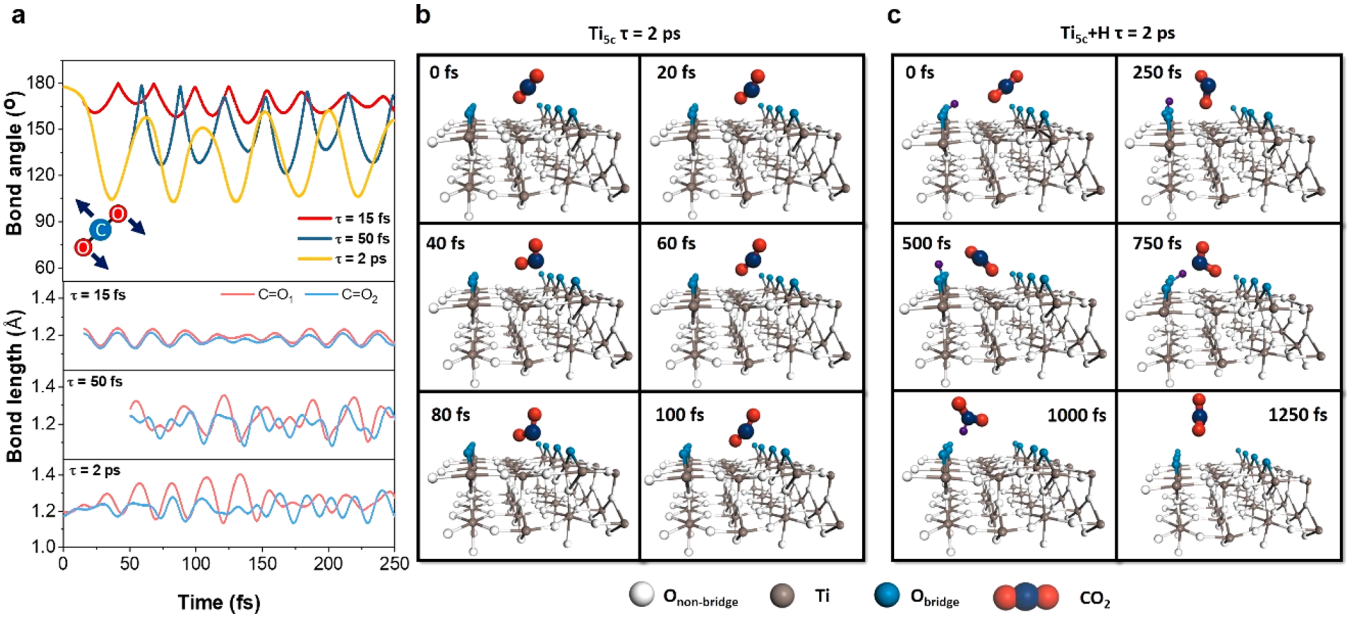

Figure 3. Specific vibrational mode excitations by the formation of transient $CO_2^{\bullet-}$ with the adsorption on Ti_{5C} on the TiO_2(110) surface. (a) O═C═O bond angle and bond length evolution with different $CO_2^{\bullet-}$ lifetimes. Two different C═O bonds ($C{=}O_1$ and $C{=}O_2$) are indicated with the red and blue lines, respectively. (b, c) Snapshots of the atomic structures during the MD trajectory for $CO_2^{\bullet-}$ with different τ.

arbitrary phase in the adiabatic wave functions, we apply a phase correction similar to the method introduced by Akimov.[33]

3. RESULTS

3.1. Vibrational Excitations Induced by the Transient $CO_2^{\bullet-}$. The static electronic structure of CO_2 on TiO_2 has been investigated in previous theoretical and experimental studies.[34−36] The LUMO of CO_2 is around 2.2 and 4.0 eV above the CBM, when it adsorbs in O_V or on the five-coordinated Ti (Ti_{5C}) atom. The electronic structures of CO_2 in O_V and on Ti_{5C} are shown in Figure S4. Since the LUMO of CO_2 is higher than the CBM, it is strongly hybridized with the TiO_2 conduction band states, and the electron attached to CO_2 will transfer back to the conduction band of TiO_2 easily. Therefore, a stable $CO_2^{\bullet-}$ is difficult to form. Yet, a transient $CO_2^{\bullet-}$ can still be generated by photoexcitation, and it can exist within a certain lifetime (represented by τ).

First, we study how the transient $CO_2^{\bullet-}$ induces the specific vibrational excitations. We begin with the CO_2 adsorption in O_V on the TiO_2(110) surface. In this case, one of the oxygen atoms in CO_2 will occupy the O_V site, as shown in Figure 2b,c. As we discussed in the Methodology part, during the MD, the

https://dx.doi.org/10.1021/jacs.9b13280
J. Am. Chem. Soc. 2020, 142, 3214−3221

lifetime of $CO_2^{\bullet-}$, τ, can be controlled using the I2S method.[23−26] Figure 2a shows the O═C═O bond angle and the C═O distance for τ = 5, 10, 15, and 20 fs. One can see that for τ = 10 and 15 fs, the bending mode is excited. We propose that the bending mode excitation is due to the repulsion between the free electron pairs on the O atoms of $CO_2^{\bullet-}$, and the O═C═O bending angle during the vibration depends significantly on the $CO_2^{\bullet-}$ lifetime. For τ = 5 fs, the bending mode is hardly excited. When τ is increased to 10 fs, the bending mode is clearly excited, and the angle changes in the range of [140, 180]°. If τ is further extended to 15 fs, the bending angle in the first two periods (the first 115 fs) varies in the range of [115, 160]°. After that, it slowly damps to the range of [135, 180]° within the first 250 fs. The bending mode excitation can be clearly seen from the snapshots in the MD trajectory in Figure 2b. In addition to the bending mode, the antisymmetric stretching mode, which is induced by the interaction of $CO_2^{\bullet-}$ with the O_V, is also excited when τ reaches 15 fs, which can be seen from the plotted two C═O bond lengths in Figure 2a. Interestingly, when τ reaches 20 fs, as shown in Figure 2a,c, enough energy is obtained from the transient $CO_2^{\bullet-}$ for the CO_2 to dissociate to form a CO on the surface within 30−40 fs, leaving an oxygen to fill the O_V. Our simulation successfully reproduces the electron-injection-induced CO_2 dissociation in O_V on the rutile TiO_2(110) surface observed in previous experiments.[35,36]

Comparing with O_V, if CO_2 is adsorbed on Ti_{5C}, the formation of transient $CO_2^{\bullet-}$ can also excite the bending mode, as shown in Figure 3a. However, without the O_V, the antisymmetric stretching mode is difficult to excite. In this case, CO_2 will not dissociate on the Ti_{5C} site even when τ is increased to 2 ps, as shown by the MD snapshots in Figure 3b. Only if there is a bridging hydroxyl, as shown in Figure 3c, the HCOO intermediate can be formed on a 1 ps time scale. Our results suggest that excitation of the antisymmetric stretching mode is required for the CO_2 dissociation. It is difficult to excite on the Ti_{5C} site, because the interaction of CO_2 with Ti_{5C} is much weaker than with O_V. (The adsorption energies of CO_2 on Ti_{5C} and O_V by the PBE functional with the vdW correction are 0.35 and 0.54 eV, respectively.) The analysis supports the conclusion that O_V is the active site on the rutile TiO_2(110) surface.[34−42]

3.2. CO_2 LUMO Stabilization Induced by the Vibrational Excitations. Excitation of the CO_2 vibrations can affect the CO_2 electronic levels and the molecule/solid level alignment through the electronic−vibrational coupling. Figure 4 shows the time-dependent energy level alignment of CO_2 on the TiO_2(110) surface when transient $CO_2^{\bullet-}$ is generated with different lifetimes τ. At the beginning of the MD trajectory, the LUMO of CO_2 locates around 2.0 eV above the CBM, which is in line with the static electronic structure. For the case of τ = 10 fs, the LUMO of CO_2 vibrates along with the bending mode (Figure 4a) within the energy range of [0.5, 2.2] eV. Then, if τ is increased to 15 fs, with a larger bending angle in the vibration, the LUMO is stabilized below the CBM within the first 10 fs, and it can be kept there in the first 150 fs. (Figure 4b) After that, along with the damping of the bending mode, the LUMO will move above the CBM again (Figure S5). When τ reaches 20 fs, similar to τ = 15 fs, the LUMO will decrease below the CBM in the first 10 fs. The dissociation happens around 30−40 fs. After the dissociation, the curve shown in Figure 4c indicates the position of the energy level due to the O atom that fills O_V.

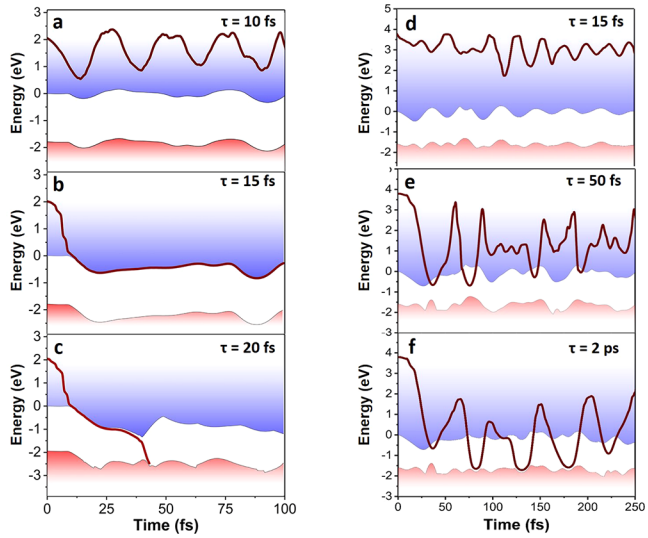

Figure 4. Evolution of the LUMO energy (red line) of CO_2 adsorption in O_v (a−c) and on Ti_{5C} (d−f) with different $CO_2^{\bullet-}$ lifetimes. The conduction and valence bands are indicated by the light blue and red shades, respectively. The zero of energy is set at the CBM.

For the case of CO_2 adsorption on Ti_{5C}, the bending of CO_2 can also stabilize the CO_2 LUMO. For τ = 50 fs and 2 ps, the LUMO of CO_2 can be stabilized below the CBM temporarily; however, without the antisymmetric vibrational mode excitation, the LUMO cannot be kept below the CBM for more than 20 fs, and CO_2 cannot dissociate.

3.3. Hot Electron Trapping by the Stabilized CO_2 LUMO. If the LUMO of CO_2 can be stabilized below the CBM, it will have a chance to trap the excited hot electrons and form a $CO_2^{\bullet-}$ again. In addition, since the LUMO is now below the CBM of TiO_2, the lifetime of the newly formed $CO_2^{\bullet-}$ will be much longer. Namely, the CO_2 can be activated in this case. We have used the NAMD simulation to check the efficiency of electron trapping by the stabilized CO_2 LUMO. The hot electron trapping dynamics with different initial energies for CO_2 in O_V are shown in Figure 5. For the case of τ = 15 fs, the population of the CO_2 LUMO on TiO_2 increases from zero to 50% within 75 fs. After trapping the photoexcited

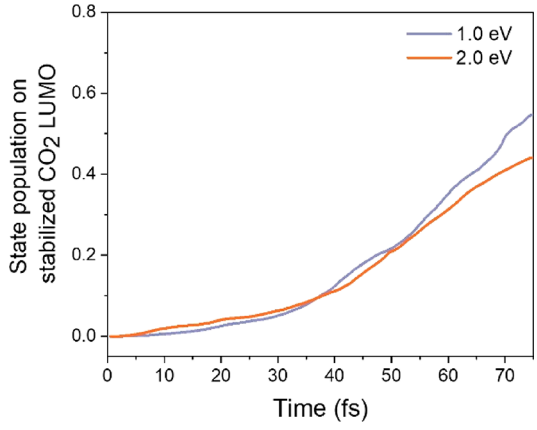

Figure 5. Hot electron trapping by stabilized CO_2 LUMO with transient $CO_2^{\bullet-}$ lifetime τ = 15 fs. The blue and orange lines represent hot electrons with different initial energies. The zero of energy is set at the CBM.

https://dx.doi.org/10.1021/jacs.9b13280
J. Am. Chem. Soc. 2020, 142, 3214−3221

electron, a $CO_2^{\bullet-}$ will be formed again. As we have discussed above, it will dissociate into CO and O to fill O_V after 30−40 fs. The hot electron trapping is difficult for CO_2 adsorbed on Ti_{5C}, since the CO_2 LUMO does not remain below the TiO_2 CBM for a sufficiently long time, as shown in Figure 4d−f.

3.4. Lifetime of the Transient $CO_2^{\bullet-}$. The discussion above leads one to conclude that the lifetime τ of the transient $CO_2^{\bullet-}$ is the critical factor governing the stabilization of the CO_2 LUMO. To understand this point better, we have performed more MD simulations using different lifetimes with τ = 5−30 fs (Table S1). We find that 12 fs is the shortest τ that can activate CO_2. Using *ab initio* NAMD, we have also investigated the $CO_2^{\bullet-}$ lifetime on O_V. The results in Figure 6

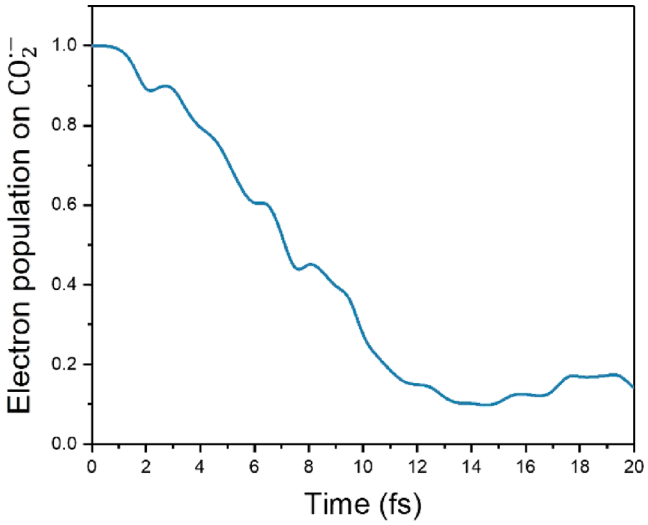

Figure 6. Lifetime of transient $CO_2^{\bullet-}$. The blue line shows the time-dependent electron population on CO_2 after a transient $CO_2^{\bullet-}$ is formed.

show that the $CO_2^{\bullet-}$ lifetime is just within 10−15 fs, which is very similar to the lifetime of the wet electron states of H_2O on TiO_2.[43] Such lifetime is just around the threshold to stabilize the CO_2 LUMO. Therefore, we propose that there exist a certain probability for the CO_2 activation through the transient $CO_2^{\bullet-}$ formation with adsorption in O_V on the TiO_2 surface.

4. DISCUSSION

The CO_2 photoreduction process induced by the transient $CO_2^{\bullet-}$ formation in O_V on the TiO_2(110) surface is summarized in Figure 7. Our results show that the bending and asymmetric stretching modes' excitations are the key factors for the CO_2 activation and reduction on TiO_2. With the adsorption in O_V and the transient $CO_2^{\bullet-}$ formation, the bending and asymmetric vibrational modes can be successfully excited, followed by the stabilization of the CO_2 LUMO, hot electron trapping, and finally the dissociation of CO_2. In this process, there are two bottlenecks: (i) The transient $CO_2^{\bullet-}$ is difficult to generate through photoexcitation. As has been discussed above, for the static CO_2, without bending mode excitation, the LUMO locates at 2.2 eV above the CBM. Therefore, to excite one electron from the valence band maximum (VBM) to the CO_2 LUMO, a photon with an energy higher than ∼5.5 eV is needed, as indicated in Figure 1a and Figure S4. Yet, if TiO_2 is n-type doped, there is an electron occupation close to the CBM.[37−39,44−47] In this case, transient

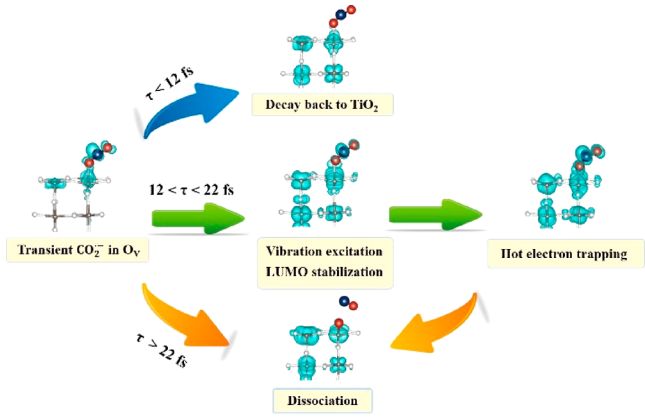

Figure 7. Schematic mapping of the CO_2 photoreduction process induced by transient $CO_2^{\bullet-}$ with different lifetimes. The charge distribution shown here is based on typical snapshots from the NAMD simulation.

$CO_2^{\bullet-}$ can be generated by photoexcitation from the CBM, with a photon energy larger than 2.2 eV. The n-type doping can be realized easily by introducing more Ti interstitials and O_V.[37−39,44−50] In fact, many experimental studies show that excitation can be generated through the defect states by O_V or Ti interstitials in TiO_2.[38,51−57] (ii) The lifetime of the transient $CO_2^{\bullet-}$ is short. As we have discussed, the lifetime of the transient $CO_2^{\bullet-}$ is within 10−15 fs, which is just at the threshold of the CO_2 LUMO stabilization requirement. The short $CO_2^{\bullet-}$ lifetime limits the efficiency of the CO_2 photoreduction on the rutile TiO_2(110) surface. Such short lifetime is due to the strong hybridization of the CO_2 orbitals with the TiO_2 electronic bands. Our results are based on the TiO_2 rutile (110) surface. We propose that, for different oxide surfaces, the $CO_2^{\bullet-}$ lifetime can be different due to varying interactions. It is also possible to tune the CO_2−oxide interaction by coadsorption of other molecules. For example, it will be very interesting to see what occurs if there is a H_2O adsorption besides CO_2.[58] Actually, Wu et al. showed recently that CO_2 and H_2O coadsorption will stimulate CO_2 photoreduction on Cu_2O.[59]

Besides the transient $CO_2^{\bullet-}$, we propose that the bending and antisymmetric stretching vibrations can be excited by other procedures. For example, if there are metal atoms or clusters on the surface, there might be charge transfer and orbital hybridization with CO_2.[60−64] In some cases, CO_2 with a bent geometry can even be formed.[9] Thus, the bending vibrations can be easily excited. In addition, the metal atoms can provide stronger interactions with CO_2, which is helpful for the antisymmetric stretching excitation. Changing the oxide surfaces may also play a role. Defects such as O_V on an oxide surface seem to be especially important for CO_2 to adsorb with a bent structure. For example, it was reported that CO_2 adsorbed in O_V on the anatase TiO_2 (101) surface with a bent geometry.[65] Chen et al. showed that CO_2 adsorbs with a bent geometry on a Bi_2O_3 nanosheet in an oxygen vacancy. Both these help the single electron transfer to form $CO_2^{\bullet-}$ and prompt the photoreduction.[9] Similar properties were also reported on the Co_3O_4 surface.[7] It has also been reported that functional ligands can facilitate bending of the CO_2 molecule.[66−68] This is an important alternative to overcome the highly unfavorable potential of the reduction of CO_2 by the single electron to form $CO_2^{\bullet-}$. The functional ligands have

https://dx.doi.org/10.1021/jacs.9b13280
J. Am. Chem. Soc. 2020, 142, 3214−3221

multiple and accessible redox states that have been shown to promote the electron transfer to the CO_2. These electron transfer dynamics can be studied precisely on the ultrafast regime, and the insights provided by our work assist in rationalizing the results of these references as well. Finally, recently developed experimental techniques, such as THz photoexcitation, can excite the vibrational modes selectively. We propose that these techniques can also be used to excite the bending and antisymmetric stretching vibrations of CO_2 to improve the CO_2 photoreduction efficiency on oxides.

5. CONCLUSION

To summarize, we have investigated the CO_2 photoreduction mechanism on the TiO_2 surface using the state-of-the-art time-dependent *ab initio* NAMD simulation. We found that excitation of the CO_2 bending and antisymmetric stretching vibrational modes can sufficiently stabilize the CO_2 LUMO that it is capable of trapping hot electrons and being reduced to $CO_2^{\bullet-}$. Such specific vibrational excitations are realized by transient $CO_2^{\bullet-}$ formation with a lifetime longer than 12 fs. The transiently trapped hot electrons can live for nearly 100 fs and allow CO_2 to dissociate to form CO within 30−40 fs after the trapping. Our results pave a way to understand the mechanism of the CO_2 photoreduction on oxide surfaces and provide valuable insights into the design of photocatalysts with high efficiencies.

■ ASSOCIATED CONTENT

Supporting Information

The Supporting Information is available free of charge at https://pubs.acs.org/doi/10.1021/jacs.9b13280.

Figures S1−S5, Table S1, and description of simulation methodologies (PDF)

■ AUTHOR INFORMATION

Corresponding Author

Jin Zhao − *ICQD/Hefei National Laboratory for Physical Sciences at the Microscale, CAS Key Laboratory of Strongly-Coupled Quantum Matter Physics, and Department of Physics and Synergetic Innovation Center of Quantum Information & Quantum Physics, University of Science and Technology of China, Hefei 230026, China; Department of Physics and Astronomy, University of Pittsburgh, Pittsburgh, Pennsylvania 15260, United States;* orcid.org/0000-0003-1346-5280; Email: zhaojin@ustc.edu.cn

Authors

Weibin Chu − *ICQD/Hefei National Laboratory for Physical Sciences at the Microscale, CAS Key Laboratory of Strongly-Coupled Quantum Matter Physics, and Department of Physics, University of Science and Technology of China, Hefei 230026, China; Department of Chemistry and Department of Physics and Astronomy, University of Southern California, Los Angeles, California 90089, United States;* orcid.org/0000-0001-5951-0337

Qijing Zheng − *ICQD/Hefei National Laboratory for Physical Sciences at the Microscale, CAS Key Laboratory of Strongly-Coupled Quantum Matter Physics, and Department of Physics, University of Science and Technology of China, Hefei 230026, China;* orcid.org/0000-0003-0022-3442

Oleg V. Prezhdo − *Department of Chemistry and Department of Physics and Astronomy, University of Southern California, Los Angeles, California 90089, United States;* orcid.org/0000-0002-5140-7500

Complete contact information is available at: https://pubs.acs.org/10.1021/jacs.9b13280

Notes

The authors declare no competing financial interest.

■ ACKNOWLEDGMENTS

We thank Z. Hu and W. Ji for fruitful discussions. J.Z. acknowledges support from the National Key Foundation of China, Department of Science and Technology, grant nos. 2017YFA0204904 and 2016YFA0200604, and the National Natural Science Foundation of China (NSFC), grant nos, 11620101003 and 11974322. Q.Z. acknowledges support from the National Natural Science Foundation of China (NSFC), grant no. 11704363. O.V.P. acknowledges funding from the U.S. National Science Foundation, CHE-1900510. The calculations were performed at the Environmental Molecular Sciences Laboratory at the PNNL, a user facility sponsored by the U.S. Department of Energy Office of Biological and Environmental Research.

■ REFERENCES

(1) Furukawa, H.; Yaghi, O. M. Storage of Hydrogen, Methane, and Carbon Dioxide in Highly Porous Covalent Organic Frameworks for Clean Energy Applications. *J. Am. Chem. Soc.* **2009**, *131* (25), 8875−8883.

(2) Sanz-Perez, E. S.; Murdock, C. R.; Didas, S. A.; Jones, C. W. Direct Capture of CO_2 from Ambient Air. *Chem. Rev.* **2016**, *116* (19), 11840−11876.

(3) Kattel, S.; Liu, P.; Chen, J. G. G. Tuning Selectivity of CO_2 Hydrogenation Reactions at the Metal/Oxide Interface. *J. Am. Chem. Soc.* **2017**, *139* (29), 9739−9754.

(4) White, J. L.; et al. Light-driven heterogeneous reduction of carbon dioxide: Photocatalysts and photoelectrodes. *Chem. Rev.* **2015**, *115*, 12888−12935.

(5) Yu, J. G.; Low, J. X.; Xiao, W.; Zhou, P.; Jaroniec, M. Enhanced Photocatalytic CO_2-Reduction Activity of Anatase TiO_2 by Coexposed {001} and {101} Facets. *J. Am. Chem. Soc.* **2014**, *136* (25), 8839−8842.

(6) Li, C. W.; Kanan, M. W. CO_2 Reduction at Low Overpotential on Cu Electrodes Resulting from the Reduction of Thick Cu_2O Films. *J. Am. Chem. Soc.* **2012**, *134* (17), 7231−7234.

(7) Gao, S.; et al. Atomic layer confined vacancies for atomic-level insights into carbon dioxide electroreduction. *Nat. Commun.* **2017**, *8*, 14503.

(8) Montoya, J. H.; et al. Materials for solar fuels and chemicals. *Nat. Mater.* **2017**, *16*, 70−81.

(9) Chen, S. C.; et al. Oxygen vacancy associated single-electron transfer for photofixation of CO_2 to long-chain chemicals. *Nat. Commun.* **2019**, *10*, 788.

(10) Gao, S.; et al. Partially oxidized atomic cobalt layers for carbon dioxide electroreduction to liquid fuel. *Nature* **2016**, *529*, 68−71.

(11) Gao, S.; et al. Ultrathin Co_3O_4 layers realizing optimized CO_2 electroreduction to formate. *Angew. Chem., Int. Ed.* **2016**, *55*, 698−702.

(12) Habisreutinger, S. N.; Schmidt-Mende, L.; Stolarczyk, J. K. Photocatalytic reduction of CO_2 on TiO_2 and other semiconductors. *Angew. Chem., Int. Ed.* **2013**, *52*, 7372−7408.

(13) Schwarz, H. A.; Dodson, R. W. Reduction potentials of CO_2^- and the alcohol radicals. *J. Phys. Chem.* **1989**, *93*, 409−414.

(14) Kresse, G.; Hafner, J. Ab initio molecular dynamics for liquid metals. *Phys. Rev. B: Condens. Matter Mater. Phys.* **1993**, *47* (1), 558−561.

(15) Kresse, G.; Hafner, J. *Phys. Rev. B: Condens. Matter Mater. Phys.* **1993**, *48*, 13115.
(16) Kresse, G.; Hafner, J. Ab-initio molecular-dynamics simulation of the liquid-metal amorphous-semiconductor transition in germanium. *Phys. Rev. B: Condens. Matter Mater. Phys.* **1994**, *49* (20), 14251−14269.
(17) Kresse, G.; Joubert, D. From ultrasoft pseudopotentials to the projector augmented-wave method. *Phys. Rev. B: Condens. Matter Mater. Phys.* **1999**, *59* (3), 1758−1775.
(18) Blochl, P. E. Projector augmented-wave method. *Phys. Rev. B: Condens. Matter Mater. Phys.* **1994**, *50* (24), 17953−17979.
(19) Perdew, J. P.; Burke, K.; Ernzerhof, M. Generalized gradient approximation made simple. *Phys. Rev. Lett.* **1996**, *77* (18), 3865−3868.
(20) Grimme, S.; Antony, J.; Ehrlich, S.; Krieg, H. A consistent and accurate ab initio parametrization of density functional dispersion correction (DFT-D) for the 94 elements H-Pu. *J. Chem. Phys.* **2010**, *132* (15), 154104.
(21) Kowalski, P. M.; Meyer, B.; Marx, D. Composition, structure, and stability of the rutile TiO_2(110) surface: Oxygen depletion, hydroxylation, hydrogen migration, and water adsorption. *Phys. Rev. B: Condens. Matter Mater. Phys.* **2009**, *79* (11), 115410−16.
(22) Chu, W. B.; Saidi, W. A.; Zheng, Q. J.; Xie, Y.; Lan, Z. G.; Prezhdo, O. V.; Petek, H.; Zhao, J. Ultrafast Dynamics of Photongenerated Holes at a CH_3OH/TiO_2 Rutile Interface. *J. Am. Chem. Soc.* **2016**, *138* (41), 13740−13749.
(23) Huang, K.; Leung, L.; Lim, T.; Ning, Z. Y.; Polanyi, J. C. Single-electron induces double-reaction by charge delocalization. *J. Am. Chem. Soc.* **2013**, *135*, 6220−6225.
(24) Ning, Z. Y.; Polanyi, J. C. Charge delocalization induces reaction in molecular chains at a surface. *Angew. Chem., Int. Ed.* **2013**, *52*, 320−324.
(25) Anggara, K.; Leung, L.; Timm, M. J.; Hu, Z. X.; Polanyi, J. C. Approaching the forbidden fruit of reaction dynamics: Aiming reagent at selected impact parameters. *Sci. Adv.* **2018**, *4*, eaau2821.
(26) Anggara, K.; et al. Bond selectivity in electron-induced reaction due to directed recoil on an anisotropic substrate. *Nat. Commun.* **2016**, *7*, 13690.
(27) Kohler, L.; Kresse, G. Density functional study of CO on Rh(111). *Phys. Rev. B: Condens. Matter Mater. Phys.* **2004**, *70* (16), 165405.
(28) Ji, W.; Lu, Z. Y.; Gao, H. Electron core-hole interaction and its induced ionic structural relaxation in molecular systems under x-ray irradiation. *Phys. Rev. Lett.* **2006**, *97* (24), 246101.
(29) Zheng, Q.; Chu, W.; Zhao, C.; Zhang, L.; Guo, H.; Wang, Y.; Jiang, X.; Zhao, J. Ab initio nonadiabatic molecular dynamics investigations on the excited carriers in condensed matter systems. *Wiley Interdiscip. Rev.: Comput. Mol. Sci.* **2019**, *9* (6), e1411.
(30) Zhang, L. L.; Zheng, Q. J.; Xie, Y.; Lan, Z. G.; Prezhdo, O. V.; Saidi, W. A.; Zhao, J. Delocalized Impurity Phonon Induced Electron-Hole Recombination in Doped Semiconductors. *Nano Lett.* **2018**, *18* (3), 1592−1599.
(31) Qiu, J.; Bai, X.; Wang, L. J. Crossing Classified and Corrected Fewest Switches Surface Hopping. *J. Phys. Chem. Lett.* **2018**, *9* (15), 4319−4325.
(32) Wang, L. J.; Qiu, J.; Bai, X.; Xu, J. B. Surface hopping methods for nonadiabatic dynamics in extended systems. *Wiley Interdiscip. Rev.-Comput. Mol. Sci.* **2019**, e1435.
(33) Akimov, A. V. A Simple Phase Correction Makes a Big Difference in Nonadiabatic Molecular Dynamics. *J. Phys. Chem. Lett.* **2018**, *9* (20), 6096−6102.
(34) Sorescu, D. C.; Lee, J.; Al-Saidi, W. A.; Jordan, K. D. CO_2 adsorption on TiO_2(110) rutile: Insight from dispersion-corrected density functional theory calculations and scanning tunneling microscopy experiments. *J. Chem. Phys.* **2011**, *134*, 104707.
(35) Tan, S. J.; et al. CO_2 dissociation activated through electron attachment on the reduced rutile tio2(110)-1 × 1 surface. *Phys. Rev. B: Condens. Matter Mater. Phys.* **2011**, *84*, 155418.
(36) Lee, J.; Sorescu, D. C.; Deng, X. Y. Electron-induced dissociation of CO_2 on TiO_2(110). *J. Am. Chem. Soc.* **2011**, *133*, 10066−10069.
(37) Diebold, U. The surface science of titanium dioxide. *Surf. Sci. Rep.* **2003**, *48*, 53−229.
(38) Henderson, M. A. A surface science perspective on TiO_2 photocatalysis. *Surf. Sci. Rep.* **2011**, *66*, 185−297.
(39) Pacchioni, G. Oxygen vacancy: The invisible agent on oxide surfaces. *ChemPhysChem* **2003**, *4*, 1041−1047.
(40) Schaub, R.; et al. Oxygen vacancies as active sites for water dissociation on rutile TiO_2(110). *Phys. Rev. Lett.* **2001**, *87*, 266104.
(41) Lin, X.; et al. Structure and dynamics of CO_2 on rutile TiO_2(110)-1 × 1. *J. Phys. Chem. C* **2012**, *116*, 26322−26334.
(42) Dohnalek, Z.; Lyubinetsky, I.; Rousseau, R. Thermally-driven processes on rutile TiO_2(110)-(1 × 1): A direct view at the atomic scale. *Prog. Surf. Sci.* **2010**, *85*, 161−205.
(43) Petek, H.; zhao, J. Ultrafast interfacial proton-coupled electron transfer. *Chem. Rev.* **2010**, *110*, 7082−7099.
(44) Onda, K.; Li, B.; Petek, H. Two-photon photoemission spectroscopy of TiO_2(110) surfaces modified by defects and O^{-2} or H_2O adsorbates. *Phys. Rev. B: Condens. Matter Mater. Phys.* **2004**, *70*, 045415.
(45) Wendt, S.; et al. Oxygen vacancies on TiO_2(110) and their interaction with H_2O and O^{-2}: A combined high-resolution stm and dft study. *Surf. Sci.* **2005**, *598*, 226−245.
(46) Schaub, R.; et al. Oxygen-mediated diffusion of oxygen vacancies on the TiO_2(110) surface. *Science* **2003**, *299*, 377−379.
(47) Pang, C. L.; Lindsay, R.; Thornton, G. Structure of clean and adsorbate-covered single-crystal rutile TiO_2 surfaces. *Chem. Rev.* **2013**, *113*, 3887−3948.
(48) Di Valentin, C.; Pacchioni, G.; Selloni, A. Electronic structure of defect states in hydroxylated and reduced rutile TiO_2(110) surfaces. *Phys. Rev. Lett.* **2006**, *97*, 166803.
(49) Wendt, S.; et al. The role of interstitial sites in the ti3d defect state in the band gap of titania. *Science* **2008**, *320*, 1755−1759.
(50) Yin, W. J.; Wen, B.; Zhou, C. Y.; Selloni, A.; Liu, L. M. Excess electrons in reduced rutile and anatase TiO_2. *Surf. Sci. Rep.* **2018**, *73*, 58−82.
(51) Onda, K.; et al. Wet electrons at the H_2O/TiO_2(110) surface. *Science* **2005**, *308*, 1154−1158.
(52) Li, B.; et al. Ultrafast interfacial proton-coupled electron transfer. *Science* **2006**, *311*, 1436−1440.
(53) Zuo, F.; et al. Self-doped Ti_{3+} enhanced photocatalyst for hydrogen production under visible light. *J. Am. Chem. Soc.* **2010**, *132*, 11856−11857.
(54) Wang, Z. Q.; et al. Localized excitation of Ti_{3+} ions in the photoabsorption and photocatalytic activity of reduced rutile TiO_2. *J. Am. Chem. Soc.* **2015**, *137*, 9146−9152.
(55) Argondizzo, A.; et al. Ultrafast multiphoton pump-probe photoemission excitation pathways in rutile TiO_2(110). *Phys. Rev. B: Condens. Matter Mater. Phys.* **2015**, *91*, 155429.
(56) Guo, Q.; Zhou, C. Y.; Ma, Z. B.; Yang, X. M. Fundamentals of TiO_2 photocatalysis: Concepts, mechanisms, and challenges. *Adv. Mater.* **2019**, *31*, 1901997.
(57) Petrik, N. G.; et al. Chemical reactivity of reduced TiO_2(110): The dominant role of surface defects in oxygen chemisorption. *J. Phys. Chem. C* **2009**, *113*, 12407−12411.
(58) Smith, R. S.; Li, Z. J.; Chen, L.; Dohnalek, Z.; Kay, B. D. Adsorption, desorption, and displacement kinetics of H_2O and CO_2 on TiO_2(110). *J. Phys. Chem. B* **2014**, *118*, 8054−8061.
(59) Wu, Y. A.; et al. Facet-dependent active sites of a single Cu_2O particle photocatalyst for CO_2 reduction to methanol. *Nat. Energy* **2019**, *4*, 957.
(60) Rasko, J. Ftir study of the photoinduced dissociation of CO_2 on titania-supported noble metals. *Catal. Lett.* **1998**, *56*, 11−15.
(61) Chang, X. X.; Wang, T.; Gong, J. L. CO_2 photo-reduction: Insights into CO_2 activation and reaction on surfaces of photocatalysts. *Energy Environ. Sci.* **2016**, *9*, 2177−2196.

https://dx.doi.org/10.1021/jacs.9b13280
J. Am. Chem. Soc. 2020, 142, 3214−3221

(62) Low, J. X.; Cheng, B.; Yu, J. G. Surface modification and enhanced photocatalytic CO_2 reduction performance of TiO_2: A review. *Appl. Surf. Sci.* **2017**, *392*, 658−686.
(63) Liu, Z. P.; Gong, X. Q.; Kohanoff, J.; Sanchez, C.; Hu, P. Catalytic role of metal oxides in gold-based catalysts: A first principles study of CO oxidation on TiO_2 supported au. *Phys. Rev. Lett.* **2003**, *91*, 266102.
(64) Gong, X. Q.; Selloni, A.; Dulub, O.; Jacobson, P.; Diebold, U. Small au and pt clusters at the anatase TiO_2(101) surface: Behavior at terraces, steps, and surface oxygen vacancies. *J. Am. Chem. Soc.* **2008**, *130*, 370−381.
(65) Ji, Y. F.; Luo, Y. New mechanism for photocatalytic reduction of CO_2 on the anatase TiO_2(101) surface: The essential role of oxygen vacancy. *J. Am. Chem. Soc.* **2016**, *138*, 15896−15902.
(66) Morris, A. J.; Meyer, G. J.; Fujita, E. Molecular Approaches to the Photocatalytic Reduction of Carbon Dioxide for Solar Fuels. *Acc. Chem. Res.* **2009**, *42* (12), 1983−1994.
(67) Sita, L. R.; Babcock, J. R.; Xi, R. Facile metathetical exchange between carbon dioxide and the divalent group 14 bisamides $M[N(SiMe_3)_2]_2$ (M = Ge and Sn). *J. Am. Chem. Soc.* **1996**, *118* (44), 10912−10913.
(68) Cole, E. B.; Lakkaraju, P. S.; Rampulla, D. M.; Morris, A. J.; Abelev, E.; Bocarsly, A. B. Using a One-Electron Shuttle for the Multielectron Reduction of CO_2 to Methanol: Kinetic, Mechanistic, and Structural Insights. *J. Am. Chem. Soc.* **2010**, *132* (33), 11539−11551.

https://dx.doi.org/10.1021/jacs.9b13280
J. Am. Chem. Soc. 2020, 142, 3214−3221